# Hybrid-polarimetry Synthetic Aperture Radar for Oil-Spill Detection

Ajeet Kumar† *Member, IEEE,*, Varsha Mishra‡ *Member, IEEE,*,
Rajib Kumar Panigrahi*, *Senior Member, IEEE,* and Marco Martorella†‡, *Fellow, IEEE,*

†National Laboratory of Radar and Surveillance Systems - CNIT, Pisa, Italy
‡University of Pisa, Pisa, Italy
*Indian Institute of Technology Roorkee, Roorkee, India
email: ajeet.kumar.in@ieee.org

***Abstract*—The Hybrid-polarimetry (hybrid-pol) Synthetic Aperture Radar (SAR) sensors are capable of providing: a sufficient amount of information about the surface that helps to accurately identify the oil-spill, and the reduced satellite revisit time that helps to efficiently monitor the oil-spill and identify minor spills before they can spread out and cause widespread damage. Based on the oil-spill descriptors derived directly from the hybrid-pol Stokes vector, we evaluated the performance of hybrid-polarimetry in separating oil-spills from clean-sea areas. For the analysis, ALOS-PALSAR L-band satellite dataset, acquired over the Gulf of Mexico, is implemented.**

***Index Terms*—Hybrid-pol, SAR, Oil-Spill, Stokes vector, ALOS-PALSAR.**

## I. Introduction

The conventional single-polarimetry (single-pol) based SAR systems transmit on one polarization (either H or V), and receive same/like polarization. These single-pol radar systems are capable of acquiring non-polarimetric or scalar information about the targets. In 1978, NASA has launched first civilian single-pol based SAR system, SEASAT, that operated in L band frequency range. Further, ERS-1 was launched by European space agency (ESA) in 1991, that was C-band single-pol based SAR system operated until March 2000. JERS-1 was another single-pol based L-band SAR system lauched by Japanese space agency (JSA) and operated in between 1992-1998. RADARSAT-1, a C-band single-pol SAR system, was launched by Canadian space agency, that operated for around 17 years since 1995. ERS-2, the followup mission of ERS-1, was launched in 1995 and operated in single-pol C-band until 2011. The NASA's Shuttle Radar Topography Mission (SRTM) satellite, operated in C- and X-band was flown on eleven day mission to generated high resolution digital topography, based on interferometry SAR (InSAR).

In single-pol SAR system, the wait time for the echoes coming from the target is sufficiently large, which helps to gain large swath coverage area. But inefficiently, the single-pol SAR system is capable of acquiring scalar information only about the target. To acquire maximum possible information about the target, the full-polarimetry (full-pol) SAR has been proposed. The first satellite based on the full-pol configuration, SIR-C/X, was launched in 1994. It was launched with the combined effort of, NASA, German space agency, and Italian space agency. The full-pol SAR system transmits two orthogonal-polarizations (H and V) in one time slot and receives pair of orthogonal-polarizations for each transmitted polarization. Two times transmission in one time slot reduces the wait time of echo coming from the target to half, that affects the swath coverage-area. Theretofore, even-though the full-pol system acquires maximum information about the target, they suffer with the drawback of having reduced swath coverage area in comparison with single-pol. This has adverse impact on satellite revisit time. However, for the application of oil-spill detection, the frequent revisit of the monitoring site is important to detect the minor spills before they can spread and cause widespread damage.

Dual-polarimetry SAR system is a trade off between single-pol and full-pol SAR systems. In a single time slot, the dual-pol system transmits one polarization and receives simultaneously two orthogonal polarizations. In comparison with full-pol, dual-pol has double swath coverage area, and in comparison with single-pol, dual-pol acquires much greater information content about the target. Further improvement in the information content of dual-pol SAR was possible by preserving the relative phase between orthogonal received wave, which lead dual-pol SAR to a novel configuration called compact-polarimetry (compact-pol) [1]. If the phase is preserved along with the intensity value, such as in compact-pol, it is possible to generate the covariance matrix and subsequently the Stokes vector. Compact-pol SAR system acquires much greater information than single-pol SAR, greater information than simple dual-pol SAR [2], and facilitates with double-swath coverage area than full-pol SAR. It is true that information content of compact-pol is not as greater as full-pol, but for some applications, the results are nearly equivalent. More specifically, the compact-pol SAR systems can be preferred over full-pol SAR in the applications where frequent monitoring of the surface is as important as the acquired amount of information content. There are broadly three types of compact-pol SAR configurations exist in literature.

- *$\pi/4$ mode*: This mode of compact-pol SAR configuration

is introduced by Souyris et. al. in 2005 [3]. In this mode, the 45° oriented linear polarization is transmitted and coherently H & V polarizations are received.

- *Dual Circular pol (DCP) mode*: The concept of DCP is first presented by Stacy-Preis in [4]. In DCP, circular wave is transmitted and two orthogonal circular waves are received.
- *Hybrid-pol mode*: The hybrid concept is first presented by R. K. Raney in [5]. It is hybrid as it transmits circular polarized wave and coherently receives two orthogonal linear polarized waves (H and V).

The dissimilarity in transmitted and received polarization avoids any chance of "like-polarization" and "cross-polarization" terms in hybrid-pol configuration, and hence prevents cross-talk and ambiguities from the stronger polarization channel spilling over into the weaker polarization channel [5]. Among all reported compact-pol configurations, the hybrid-pol is happen to be superior that inherits the properties of lower losses, less mass and less RF hardware which makes hybrid-pol SAR systems most suitable SAR configuration for the application of oil-spill detection.

## II. Hybrid-pol based oil-Spill descriptors

Various studies presented in open literature have demonstrated the rich potential of hybrid-pol SAR that motivates us to carry out further analysis [5]–[21]. Specifically, R. K. Raney has promoted the use of the hybrid-pol SAR through his works and proven that the analysis of hybrid-pol data can be started through the Stokes parameters generated from the received back-scattered wave. The hybrid-pol Stokes parameters can be represented as follows:

$$[S] = \begin{bmatrix} G_0 \\ G_1 \\ G_2 \\ G_3 \end{bmatrix} = \begin{bmatrix} \langle |E_{RH}|^2 + |E_{RV}|^2 \rangle \\ \langle |E_{RH}|^2 - |E_{RV}|^2 \rangle \\ 2Re\langle E_{RH} E_{RV}^* \rangle \\ -2Im\langle E_{RH} E_{RV}^* \rangle \end{bmatrix} \tag{1}$$

where, $[S]$ indicates Stokes vector, $G_0$ to $G_4$, indicate four Stokes parameters, and $E_{RH}$ and $E_{RV}$ indicate the received electric field. By utilizing the Stokes parameters directly for the analysis, few hybrid-pol decomposition methods, such as $m-\delta$ [22], $m-\alpha$ [23], $m-\chi$[24], and $HTM$ [16] methods, are reported in literature. Among these approaches, the $HTM$ introduces hybrid-pol model based approach in its complete form that estimates surface-, dihedral-, and volume-scattering mechanisms by using scattering models with surface dielectrics. The $HTM$ method establishes a framework to utilize Freeman-Durden's [25] volume scattering model and Yamaguchi's volume scattering model [26] to establish the three-component hybrid-pol decomposition model. Further extensions in hybrid-pol model-based decomposition method are carried out in [27] and [28], by advancing the $HTM$ approach and utilizing more efficient volume scattering models. The utilization of $HTM$ theory has also been seen in estimating the dielectric constant of lunar surface, based on Chandrayaan-2 hybrid-pol SAR data [17]. Although, the utilization of these decomposition approaches in oil-spill detection is subject to future implementation. The launch of future joint ISRO-NASA mission, i.e. NISAR will open the possibility in this direction [29]. For the time being, the prevalent approach in hybrid-polarimetry is to utilize the rich literature of full-polarimetry and establish the hybrid-pol version of the well established full-pol oil-spill descriptors. In this paper, we tried to perform the comparative evaluation on these descriptors based their behavior in oil-spilled and oil-free regions. For the evaluation, the following parameters are taken under consideration for the analysis.

*1) $\gamma_{CTLR}$:* The parameter $\gamma_{CTLR}$ is a hybrid-pol approximation of the full-polarimetry parameter indicating correlation between single-bounce and double-bounce scattering mechanism [30], [31]. This parameter is a direct indication of surface-roughness, and hence, exhibits higher value for clean-sea regions while lower value for damped oil-spill regions. In terms of hybrid-pol stokes parameter, the $\gamma_{CTLR}$ can be represented as:

$$\gamma_{CTLR} = \sqrt{\frac{G_1^2 + G_2^2}{G_0^2 - G_3^2}} \tag{2}$$

*2) Conformity-Coefficient:* The hybrid-pol version of the Conformity-coefficient ($\mu_{cc}$) is derived by Turong-Loi *et. al.* in [32]. For the expression and complete derivation on this parameter, one can refer to [32]. Although, Zhang *et al.* have first time demonstrated that $\mu_{cc}$ can be utilized for oil-spill detection [9]. The value of this parameter is expected to be positive for clean-sea areas, whereas, negative for oil-spilled areas [9].

*3) Coherence Parameter:* Hybrid-pol based parameters, such as degree-of-polarization, conformity index ($\mu$), ellipticity parameter, coherence Parameter ($C_{oh}$), etc., are implemented in [7], [10] for oil-spill detection. Among these, the $C_{oh}$ is declared best in separating oil-covered with clean-sea surfaces [10]. Therefore we included this parameter here for the analysis. The complete details on the establishment of this parameter in terms of hybrid-pol data can be found in [10].

*4) Phase angle ($\delta$):* The phase angle ($\delta$) based an unsupervised classifier is proposed in [33] for separating the oil-spill and oil-free regions. This parameter has a capability to separate single-bounce scattering generated from clean-sea region with multiple-scattering, generated from oil-spilled region. The $\delta$ parameter in terms of hybrid-pol data, can be expressed as

$$\delta = \tan^{-1}\left(\frac{G_3}{G_2}\right) \tag{3}$$

*5) Correlation-Coefficient ($\rho_{CL}$):* The parameter $\rho_{CL}$ is hybrid-pol version of the full-pol correlation-coefficient parameter $\rho_{HV}$ described in [10]. For clean sea area, when Bragg Scattering dominates, the value of $\rho_{CL}$ is expected to be high and close to one. Conversely, for the oil-spilled region, the value of $\rho_{CL}$ is expected to be very low [10].

## III. Results and Analysis

The hybrid-polarimetry data synthesized from the real L-band ALOS-PALSAR full-polarimetry data is used for the

evaluation. The implemented data contains actual oil-spilled and oil-free regions in the ocean Gulf of Mexico region [34]. For the visual interpretation, the RGB image is shown in Fig. 1. The clean-sea as well as oil-spilled regions are taken under consideration for the analysis, which are indicated by red rectangles on Fig. 1. The oil-spill descriptors, as discussed in Section II, are analyzed over these regions. The histogram plots of these descriptors are produced separately for clean-sea and oil-spilled regions, and added in Fig. 2. One can observe visually the difference in the histograms of clean-sea and oil-spilled regions. Moreover, to perform more clear quantitative evaluation, the normalized distance between the histograms are calculated for each of the corresponding parameters. The normalized distance ($d_n$), with the help of: mean of histogram in oil-spilled ($\mu_{OS}$), mean of histogram in clean-sea ($\mu_{CS}$), variance of histogram in oil-spilled ($\sigma_{OS}$), and variance of histogram in clean-sea ($\sigma_{OS}$), can be calculated as

$$d_n = |\mu_{OS} - \mu_{CS}|/(\sigma_{OS} + \sigma_{CS}) \tag{4}$$

Based on the normalized distance of separation ($d_n$) shown in Fig. 2, it is worth to observe that the conformity coefficient and correlation-coefficient perform much better in separating the oil-spilled area from the clean-sea regions, whereas, the phase angle ($\delta$) and $\gamma_{CTLR}$ obtains very poor separation between oils-pilled and clean sea region. The Coherence Parameter performs moderate here.

## IV. Conclusion

The ALOS-PALSAR L-band dataset of Gulf of Mexico region is implemented to analyze the performance of oil-spill descriptors derived from the hybrid-pol data. Among five implemented descriptor, the two: conformity coefficient and correlation-coefficient, performs optimum and can be implemented in future for separating the oil-spill from clean-sea area. Although, further analysis with other datasets and more derived descriptors are due for the future extension of this work.

## Acknowledgment

The work of this paper is supported by National Inter-University Consortium for Telecommunications (CNIT, www.cnit.it), and carried out at Radar and Surveillance Systems (RaSS) National Laboratory of CNIT.

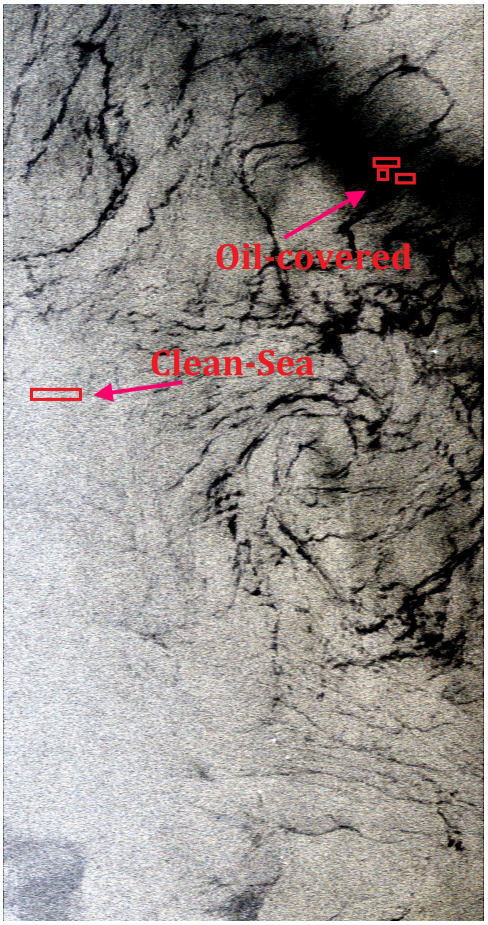


Figure 1. RGB image of ALOS-PALSAR data of ID: Data Id: ALP-SRP104460550, containing Oil-Covered and Clean-Sea regions marked with red rectangles.

## References

[1] R. K.Raney, "Dual-polarized SAR and Stokes parameters," *IEEE Geoscience and Remote Sensing Letters*, vol. 3. NO.3, pp. 317–319, July 2006.

[2] F. J. Charbonneau, B. Brisco, R. K. Raney, H. McNairn, C. Liu, P. W. Vachon, J. Shang, R. DeAbreu, A. M. C. Champagne, and T. Geldsetzer, "Compact polarimetry overview and applications assessment," *Canadian Journal of Remote Sensing*, vol. 36, Suppl. 2, pp. S298–S315, 2010.

[3] J.-C. Souyris, P. Imbo, R. Fjortoft, S. Mingot, and J.-S. Lee, "Compact Polarimetry Based on Symmetry Properties of Geophysical Media: The $\pi/4$ Mode," *IEEE Transaction on Geoscience and Remote Sensing*, vol. 43. NO.3, pp. 634–646, March 2005.

[4] N. Stacy and M. Preiss, "Compact polarimetric analysis of X-band SAR data," *in Proc. EUSAR, Germany*, May 2006.

[5] R. K. Raney, "Hybrid-polarity SAR architecture," *IEEE Transaction on Geoscience and Remote Sensing*, vol. 45,No.11, pp. 3397–3404, Nov. 2007.

[6] A. Kumar and R. K. Panigrahi, "Oil-spill detection using hybrid-pol data through reconstruction technique," *Electronics Letters*, vol. 55, no. 9, pp. 558–561, 2019.

[7] R. Shirvany, M. Chabert, and J. Y. Tourneret, "Ship and oil-spill detection using the degree of polarization in linear and hybrid/compact dual-pol SAR," *IEEE Journal of selected topics in applied Earth observations and remote sensing*, vol. 5, no. 3, pp. 885–892, Jun. 2012.

[8] Y. Li, Y. Zhang, J. Chen, and H. Zhang, "Improved compact polarimetric SAR quad-pol reconstruction algorithm for oil spill detection," *IEEE Geoscience and Remote Sensing Letter*, vol. 11, no. 6, pp. 1139–1142, Jun. 2014.

[9] B. Zhang, W. Perrie, X. Li, and W. G. Pichel, "Mapping sea surface oil slicks using RADARSAT-2 quad-polarization SAR image," *Geophysical Research Letters*, vol. 38, no. 10, pp. 1–5, May 2011.

[10] A. Salberg, . Rudjord, and A. H. S. Solberg, "Oil spill detection in hybrid-polarimetric SAR images," *IEEE Transactions on Geoscience and Remote Sensing*, vol. 52, no. 10, pp. 6521–6533, Oct. 2014.

[11] M. J. Collins, M. Denbina, B. Minchew, C. E. Jones, and B. Holt, "On the use of simulated airborne compact polarimetric SAR for characterizing oil-water mixing of the Deepwater Horizon oil spill," *IEEE Journal of Selected Topics in Applied Earth Observations and Remote Sensing*, vol. 8, no. 3, pp. 1062–1077, Mar. 2015.

[12] R. K. Raney, J. T. S. Cahill, G. W. Patterson, and D. B. J. Bussey, "The $m - \chi$ decomposition of hybrid dual-polarimetric radar data," *Geoscience and Remote Sensing Symposium (IGARSS)*, pp. 5093–5096, Jul. 2012.

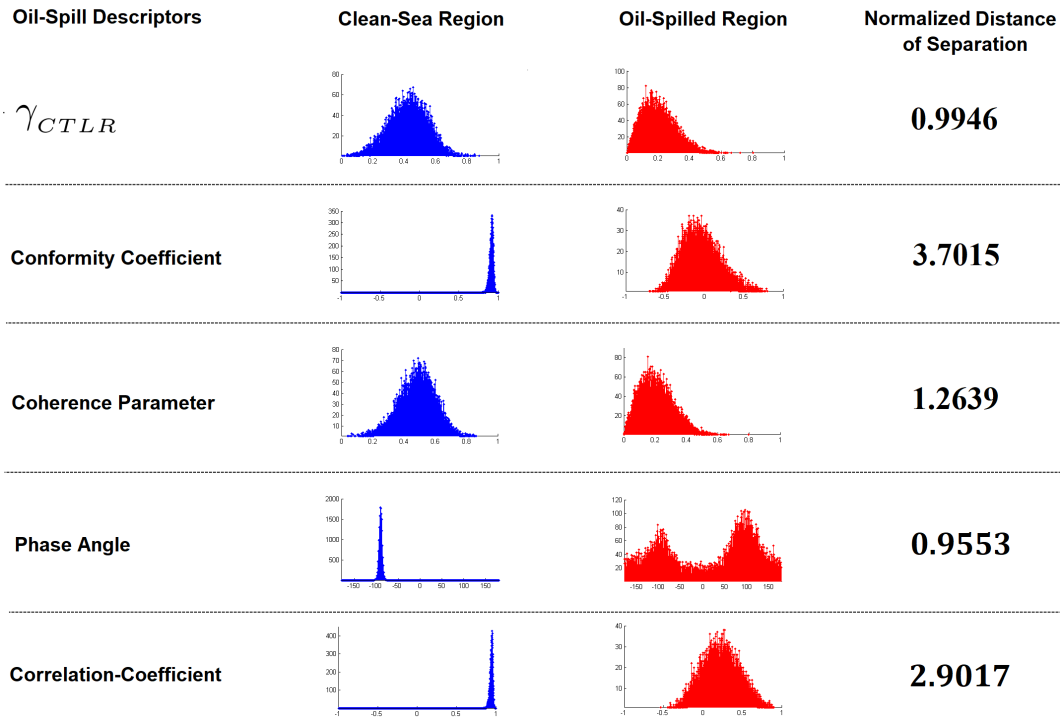


Figure 2. Histogram-based performance analysis of hybrid-pol oil-spill descriptors.


[13] S. R. Cloude, D. G. Goodenough, and H. Chen, "Compact decomposition theory," *IEEE Geoscience and Remote Sensing Letter*, vol. 9,NO.1, pp. 28–32, Jan. 2012.

[14] M. L. Truong-Loï¿œ, A. Freeman, P. C. Dubois-Fernandez, and E. Pottier, "Estimation of soil moisture and Faraday rotation from bare surfaces using compact polarimetry," *IEEE Transaction on Geoscience and Remote Sensing*, vol. 47, NO.11, pp. 3608–3615, Nov. 2009.

[15] R. K. Panigrahi and A. K. Mishra, "Unsupervised classification of scattering behaviour using hybrid-polarimetry," *IET Radar, Sonar and Navigation*, vol. 7,Iss.3, pp. 270–276, 2013.

[16] A. Kumar, A. Das, and R. K. Panigrahi, "Hybrid-pol based three-component scattering model for analysis of RISAT data," *IEEE Journal of Selected Topics in Applied Earth Observations and Remote Sensing*, vol. 10, no. 12, pp. 5155–5162, Dec. 2017.

[17] A. Kumar, I. M. Kochar, D. K. Pandey, A. Das, D. Putrevu, R. Kumar, and R. K. Panigrahi, "Dielectric constant estimation of lunar surface using Mini-RF and Chandrayaan-2 SAR data," *IEEE Transactions on Geoscience and Remote Sensing*, vol. 60, pp. 1–8, 2022.

[18] A. Kumar, R. K. Panigrahi, and A. Das, "Three-component decomposition technique for hybrid-pol sar data," *IET Radar, Sonar & Navigation*, vol. 10, no. 9, pp. 1569–1574, 2016.

[19] A. Kumar and R. K. Panigrahi, "Classification of hybrid-pol data using novel cross-polarisation estimation approach," *Electronics Letters*, vol. 54, no. 3, pp. 161–163, Feb. 2018.

[20] A. K. and R. K. Panigrahi, "Entropy based reconstruction technique for analysis of hybrid-polarimetric sar data," *IET Radar, Sonar Navigation*, vol. 13, no. 4, pp. 620–626, 2019.

[21] A. Kumar, A. Das, and R. K. Panigrahi, "Hybrid-pol decomposition methods: A comparative evaluation and a new entropy-based approach," *IETE Technical Review*, vol. 37, no. 3, pp. 296–308, 2020.

[22] R. K. Raney, "Hybrid-polarity SAR architecture," *IEEE Transaction on Geoscience and Remote Sensing*, vol. 45, no. 11, pp. 3397–3404, Nov. 2007.

[23] S. R. Cloude, D. G. Goodenough, and H. Chen, "Compact decomposition theory," *IEEE Geoscience and Remote Sensing Letter*, vol. 9, no. 1, pp. 28–32, Jan. 2012.

[24] R. K. Raney, J. T. S. Cahill, G. W. Patterson, and D. B. J. Bussey, "The $m-\chi$ decomposition of hybrid dual-polarimetric radar data," *Geoscience and Remote Sensing Symposium (IGARSS)*, pp. 5093–5096, Jul. 2012.

[25] A. Freeman and S. L. Durden, "A three-component scattering model for polarimetric SAR data," *IEEE Transaction on Geoscience and Remote Sensing*, vol. 36, no.3, pp. 963–973, May 1998.

[26] Y. Yamaguchi, T. Moriyama, M. Ishido, and H. Yamada, "Four-component scattering model for polarimetric SAR image decomposition," *IEEE Transaction on Geoscience and Remote Sensing*, vol. 43, no. 8, pp. 1699–1706, Aug. 2005.

[27] K. Inderkumar, A. Kumar, and R. K. Panigrahi, "Three-component decomposition of hybrid-polsar data with volume scattering models," *IEEE Access*, vol. 9, pp. 117 415–117 423, 2021.

[28] W. Hou, F. Zhao, X. Liu, and R. Wang, "General two-stage model-based three-component Hybrid compact polarimetric SAR decomposition method," *IEEE Journal of Selected Topics in Applied Earth Observations and Remote Sensing*, vol. 14, pp. 4647–4660, 2021.

[29] A. technical Report on, "Protecting water, land, and people from oil spills," NASA, https://nisar.jpl.nasa.gov/system/documents/files/9_NISAR_Applications_OilSpills1.pdf, [Accessed: 2022-08-31].

[30] I. Hajnsek, E. Pottier, and S. Cloude, "Inversion of surface parameters from polarimetric sar," *IEEE Transactions on Geoscience and Remote Sensing*, vol. 41, no. 4, pp. 727–744, 2003.

[31] J. Yin, J. Yang, Z.-S. Zhou, and J. Song, "The extended Bragg scattering model-based method for ship and oil-spill observation using compact polarimetric SAR," *IEEE Journal of Selected Topics in Applied Earth Observations and Remote Sensing*, vol. 8, no. 8, pp. 3760–3772, 2015.

[32] M. L. Truong-Loi, A. Freeman, P. C. Dubois-Fernandez, and E. Pottier, "Estimation of soil moisture and Faraday rotation from bare surfaces using compact polarimetry," *IEEE Transaction on Geoscience and Remote Sensing*, vol. 47, no. 11, pp. 3608–3615, Nov. 2009.

[33] B. Zhang, X. Li, W. Perrie, and O. Garcia-Pineda, "Compact polarimetric synthetic aperture radar for marine oil platform and slick detection," *IEEE Transactions on Geoscience and Remote Sensing*, vol. 55, no. 3, pp. 1407–1423, Mar. 2017.

[34] M. Migliaccio, F. Nunziata, A. Montuori, X. Li, and W. G. Pichel, "A multifrequency polarimetric SAR processing chain to observe oil fields in the Gulf of Mexico," *IEEE Transactions on Geoscience and Remote Sensing*, vol. 49, no. 12, pp. 4729–4737, Dec. 2011.